Bonding Mechanism and Atomic Geometry of an Ordered Hydroxyl Overlayer on Pt(111)

Ari P. Seitsonen,[†,‡] Yingjie Zhu,[†] Kolja Bedürftig,[†] and Herbert Over*[,†]

Contribution from the Department of Physical Chemistry, Fritz-Haber-Institut der MPG, Faradayweg 4-6, D-14195 Berlin, Germany, and INFM, Unità di Roma, Dipartimento di Fisica, Università La Sapienza, P.'le A. Moro 2, I-00185 Roma, Italy

Received January 9, 2001. Revised Manuscript Received May 24, 2001

Abstract: Exposing water to a (2×2)−O precovered Pt(111) surface at 100 K and subsequently annealing at 155 K led to the formation of a well-ordered $(\sqrt{3} \times \sqrt{3})R30°$ overlayer. The structure of this overlayer is determined by DFT and full dynamical LEED calculations. There are two O containing groups per $(\sqrt{3} \times \sqrt{3})R30°$ unit cell and both occupy near on-top positions with a Pt−O bond length of (2.11 ± 0.04) Å. DFT calculations determined the hydrogen positions of the OH species and clearly indicate hydrogen bonds between the neighboring adsorbed OH groups whose interaction is mainly of electrostatic nature. A theoretical comparison with H_2O shows the hybridization of OH on Pt(111) to be sp^3.

Introduction

Fisher and Sexton first demonstrated by high-resolution electron energy loss spectroscopy (HREELS) and ultraviolet photoelectron spectroscopy (UPS) the formation of hydroxyl species when water molecules dissociate over an atomic oxygen pre-covered Pt(111) surface at a sample temperature above 150 K.[1] Water adsorbs molecularly on the clean Pt(111) surface at 100 K and desorbs between 120 and 150 K.[2] Obviously preadsorbed atomic oxygen on the Pt(111) surface promotes the dissociation of water. This finding is of particular significance, as the direct observation of reaction intermediates in the catalytic hydrogen oxidation reaction, such as the hydroxyl species, has proven to be difficult. Further evidence for the existence of adsorbed OH species on Pt(111) was reported later.[2−4] White and co-workers suggested that the coadsorption of H_2O and O results in a mixed OH + H_2O rather than a pure OH overlayer on Pt(111).[5]

Unfortunately, the spectroscopic studies have led to controversial interpretation and speculation concerning the atomic geometry of the hydroxyl overlayer on Pt(111). The adsorption of OH in 3-fold hollow sites was suggested in refs 6 and 7. More recently, the on-top position for OH adsorption was proposed on the basis of a combined HREELS and scanning tunneling microscopy (STM) study.[8] This unclear situation has therefore called for a detailed structural analysis.

Here we report about the first structure determination of an OH overlayer on a metal surface, i.e., Pt(111), by employing density functional theory (DFT) calculations and quantitative low-energy electron diffraction (LEED). The resulting surface structure and the binding mechanism are elucidated by DFT calculations.

Experimental and Calculational Section

The experiments were conducted in a UHV chamber (base pressure: 1×10^{-10} mbar) equipped with display-type four-grid LEED optics and with standard facilities for surface cleaning and characterization. LEED intensity data were taken with a highly sensitive camera system to minimize damage from the OH overlayer by electron irradiation. Details of the experimental setup can be found elsewhere.[9] To clean the sample, the Pt(111) sample was annealed at 1273 K for 10 min, followed by oxidation at 973 K in O_2 (5×10^{-8} mbar) for 30 min. The sample was then treated by argon ion sputtering (Ar pressure, 3×10^{-5} mbar; energy, 500 eV) for 10 min. Finally, the sample was flashed to 1173 K to anneal the surface followed by cooling to room temperature. This cleaning procedure was repeated several times until no impurities were detected by AES, and the (1×1) LEED pattern of Pt(111) was sharp and with low background intensity. We should mention that we used the same Pt(111) sample as in ref 8 as it allows direct comparison of the results in ref 8 with those presented here.

The (2×2)−O precovered Pt(111) surface was prepared by exposing the clean Pt(111) surface to 2.2 L of oxygen at 100 K. The sample was then annealed at 200 K for 30 s. This produces a well-ordered (2×2)−O overlayer on Pt(111) as indicated by LEED. Water was exposed to the (2×2)-O precovered Pt(111) surface (water pressure, 6.5×10^{-9} mbar; 10 min) at a sample temperature of 100 K. Finally, the sample was annealed at 155 K for 2 min, resulting in a well-ordered (hydroxyl) overlayer on Pt(111) with a nice $(\sqrt{3} \times \sqrt{3})R30°$ LEED pattern.

The LEED I−V measurements were carried out in the energy range from 40 to 350 eV in steps of 1 eV at normal incidence and at a sample temperature of 100 K, running the cryostat with liquid nitrogen. The primary electron beam was reduced to 100 nA. The complete LEED data set was recorded by a computer-controlled, highly sensitive CCD camera system (SensiCam). The data acquisition took only 2 min so that no degradation of the OH overlayer took place. After the LEED data were taken, we checked with thermal desorption spectroscopy

* Authors to whom correspondence should be addressed. Fax: +49-711 689 1010. E-mail: Ari.P.Seitsonen@iki.fi, H.Over@fkf.mpg.de.
† Fritz-Haber-Institut der MPG.
‡ Università La Sapienza.

(1) Fisher, G. B.; Sexton, B. A. *Phys. Rev. Lett.* **1980**, *44*, 683.
(2) Fisher, G. B.; Gland, J. L. *Surf. Sci.* **1980**, *94*, 446.
(3) Creighton, J. R.; White, J. M. *Surf. Sci.* **1982**, *122*, L648.
(4) Melo, A. V.; O'Grady, W. E.; Chottiner, G. S.; Hoffman, R. W. *Appl. Surf. Sci.* **1985**, *21*, 160.
(5) Mitchell, G. E.; Akhter, S.; White, J. M. *Surf. Sci.* **1986**, *166*, 283.
(6) Mitchell, G. E.; White, J. M. *Chem. Phys. Lett.* **1987**, *135*, 84.
(7) Gilarowski, G.; Erley, W.; Ibach, H. *Surf. Sci.* **1996**, *351*, 156−164.
(8) Bedürftig, K.; Völkening, S.; Wang, Y.; Wintterlin, J.; Jacobi, K.; Ertl, G. *J. Chem. Phys.* **1999**, *111*, 11147−11154.
(9) Over, H.; Bludau, H.; Skottke-Klein, M.; Ertl, G.; Moritz, W.; Campbell, C. T. *Phys. Rev. B* **1992**, *45*, 8638−8649.

10.1021/ja015525l CCC: $20.00
Published on Web 07/07/2001

(TDS) that indeed only OH was present on the Pt(111) surface. All data evaluation was performed off-line. The LEED intensity versus energy curves (LEED I−V curves) were generated for each individual diffraction beam by integrating the spot intensity and properly subtracting of the background intensity. Data processing includes intensity normalization to the incident electron current, smoothening, and averaging over symmetry-equivalent beams. This procedure resulted in a data set containing four nonequivalent integral-order and six nonequivalent fractional-order beams. The total energy range of the LEED I−V curves was 1200 eV. LEED I−V curves were computed using the program code of Moritz[10] and compared with the experimental LEED I−V curves by employing a least-squares optimization scheme[11,12] based on Pendry's *r*-factor R_P.[13] LEED I−V data are known to contain surface structural information similar to X-ray diffraction data which reveals bulk structure information of crystalline materials.[14]

For the DFT calculations we employed the generalized gradient approximation of Perdew et al.[15] for the exchange-correlation functional. We used a plane wave basis set with an energy cutoff of 50 Ry and ab initio pseudopotentials in the fully separable form for O and Pt;[16] for hydrogen a $-1/r$ potential was used. The surface was modeled by a supercell containing a four-layer slab of Pt(111) and a $(\sqrt{3} \times \sqrt{3})$-R30° overlayer of OH on one side of the slab.[17] Consecutive slabs were separated by a vacuum region of about 16 Å. The integral over the Brillouin zone was performed using a special k point set[18] with 12 k points in the irreducible part of the $(\sqrt{3} \times \sqrt{3})$R30° Brillouin zone. Fermi broadening of the occupation numbers was used with a width of 0.1 eV, and the energies were extrapolated to zero temperature. We relaxed the positions of the O, H, and the first-layer Pt atoms. The lattice parameter ($a = 4.02$ Å) of Pt(111) was determined via DFT optimization of the corresponding bulk Pt and compares favorably well with the experimental value of $a = 3.92$ Å. A simple model for simulating STM images goes back to Tersoff and Hamann[19] in which the tunneling current is proportional to the density of states at the Fermi energy of the surface; this approximation assumes an *s*-like electronic state of the tip dominating the tunneling process. We simulated the operation of the scanning tunneling microscope in the constant current mode, i.e., we show the interpolated height distribution above the surface where the energy-restricted ($E_F - 0.5$ eV $< E < E_F + 0.5$ eV; E_F = Fermi energy) density remains constant. We chose a value for the constant density that corresponds to the density about 6−7 Å above the surface, a realistic value for the tip−surface distance in STM experiments.

Results and Discussion

The coadsorption of water onto a (2×2)−O precovered Pt(111) at 100 K, followed by annealing at 155 K, leads to the formation of a new overlayer with a sharp $(\sqrt{3} \times \sqrt{3})$R30° LEED pattern. In the LEED calculations, hydrogen atoms were not included so that the hydroxyl species were modeled as bare oxygen atoms. This approximation is justified by the vanishingly small scattering cross section of hydrogen atoms and has been widely used for the structure determination of adsorbed hydrocarbons.[20] Therefore, the surface structure determined by LEED will provide only the atomic geometry of the O skeleton of the $(\sqrt{3} \times \sqrt{3})$R30° overlayer including possible relaxations in the Pt(111) surface.

Table 1. The Optimum R_P Factors for Various Structural Models of the $(\sqrt{3} \times \sqrt{3})$R30° Hydroxyl Overlayer on Pt(111)

adsorption site	no. of OH[a]	R_P
on-top	2	0.29
on-top	1	0.42
bridge	2	0.81
bridge	1	0.71
fcc-hollow	2	0.65
fcc-hollow	1	0.65
hcp-hollow	2	0.86
hcp-hollow	1	0.86

[a] Number of OH groups in the unit cell.

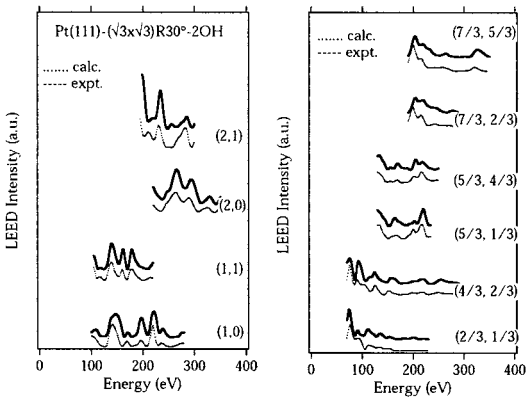

Figure 1. Comparison between experimental and calculated LEED I−V curves for the best-fit geometry of the Pt(111)−$(\sqrt{3} \times \sqrt{3})$R30°−2OH phase. The overall Pendry's *r*-factor (R_P) is 0.29.

Several structural models with one and two OH groups per $(\sqrt{3} \times \sqrt{3})$R30° unit cell were tested in the LEED simulations. We calculated the LEED I−V curves for various high-symmetry adsorption sites of the OH group: on-top, fcc-hollow, hcp-hollow, and bridge. The optimum R_P-factors for each structural model are listed in Table 1, and based on these values we can safely rule out all adsorption sites but the on-top position, as the corresponding R_P-factors are higher than 0.65. Among the two structural models for the on-top adsorption, R_P clearly favors the model with two (instead of one) OH groups per $(\sqrt{3} \times \sqrt{3})$R30° unit cell. The assignment of the on-top oxygen species to OH is based on previous HREELS measurements[8] and the fact that adsorbed oxygen atoms always occupy high-coordination sites on unreconstructed surfaces.[21] The computed LEED I−V curves for the best-fit geometry of the Pt(111)−$(\sqrt{3} \times \sqrt{3})$R30°−2OH phase are depicted in Figure 1 together with the experimental LEED I−V curves. The agreement between experimental and calculated LEED intensity data is quantified by an overall Pendry *r*-factor (R_P) of 0.29.

Figure 2 shows the optimum atomic geometry of the Pt(111)−$(\sqrt{3} \times \sqrt{3})$R30°−2OH structure, as obtained from the LEED analysis. The actual H positions are determined by DFT calculations, supposing that only OH molecules are present on the surface (this assumption is justified by HREELS measurements[8]). In the $(\sqrt{3} \times \sqrt{3})$R30° unit cell there are two adjacent OH groups at the near on-top adsorption sites. The DFT calculations indicate that the O−H bond is tilted from the surface normal by 75.8° with an O−H bond length of 1.00 Å. Structural parameter values obtained by DFT calculations are included in Figure 2.

(10) Moritz, W. *J. Phys. C* 1983, *17*, 353.
(11) Kleinle, G.; Moritz, W.; Ertl, G. *Surf. Sci.* **1990**, *226*, 119.
(12) Over, H.; Ketterl, U.; Moritz, W.; Ertl, G. *Phys. Rev. B* **1992**, *46*, 15438−15446.
(13) Pendry, J. B. *J. Phys. C* **1980**, *13*, 937.
(14) Heinz, K. *Rep. Prog. Phys.* **1995**, *58*, 637 and references therein.
(15) Perdew, J. P.; Burke, K.; Ernzerhof, M. *Phys. Rev. Lett.* **1996**, *77*, 3865−3868.
(16) Troullier, N.; Martins, J. L. *Phys. Rev. B* **1991**, *43*, 1993−2006.
(17) The difference of the asymptotic potentials at the two different surfaces of the slab due to the adsorbate was corrected using a compensating dipole layer in the vacuum. (a) Neugebauer, J.; Scheffler, M. *Phys. Rev. B* **1992**, *46*, 16067−16080. (b) Bengtsson, L. *Phys. Rev. B* **1999**, *59*, 12301−12304.
(18) Cunningham, S. L. *Phys. Rev. B* **1974**, *10*, 4988.
(19) Tersoff, J.; Hamann, D. R. *Phys. Rev. B* **1985**, *31*, 805−813.
(20) Ogletree, D. F.; Van Hove, M. A.; Somorjai, G. A. *Surf. Sci.* **1987**, *183*, 1.
(21) Over, H. *Prog. Surf. Sci.* **1998**, *58*, 249.

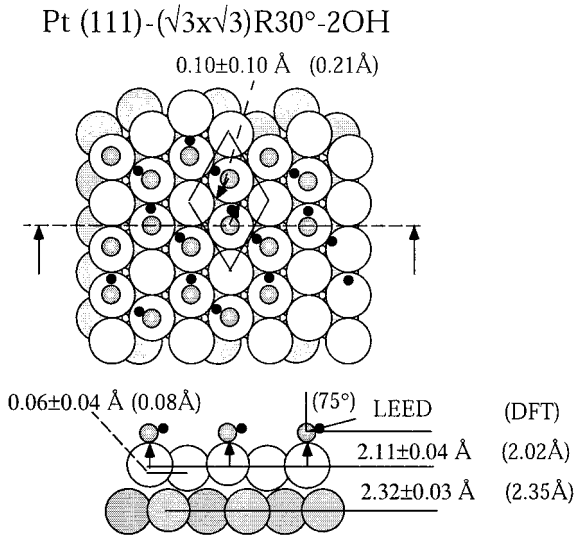

Figure 2. Top view and side view of the optimum atomic geometry of the Pt(111)−($\sqrt{3} \times \sqrt{3}$)R30°−2OH overlayer with two OH groups both sitting at near on-top sites. The distances are given in angstroms. The LEED analysis is only sensitive to the O positions. The hydrogen positions were determined by DFT calculations, assuming that two OH molecules are in the ($\sqrt{3} \times \sqrt{3}$)R30° unit cell.

The bond length of Pt−O is (2.11 ± 0.04) Å in Pt(111)−($\sqrt{3} \times \sqrt{3}$)R30°−2OH, and is increased by 0.09 Å compared to that of the Pt(111)−(2 × 2)−O phase with oxygen atoms residing in fcc sites.[22] Our DFT calculations of Pt(111)−($\sqrt{3} \times \sqrt{3}$)R30°−2OH yielded a Pt−O bond length of only 2.03 Å, which is shorter than the experimentally determined one. Very recently Michaelides and Hu argued that the Pt(111)−($\sqrt{3} \times \sqrt{3}$)R30°−2OH overlayer is a mixed ($\sqrt{3} \times \sqrt{3}$)R30°−H_2O+OH.[23] They found Pt−O bond lengths of 2.11 and 2.17 Å for OH−Pt and H_2O−Pt, respectively, which are in better agreement with our LEED results. Therefore, it might be conceivable that the ($\sqrt{3} \times \sqrt{3}$)R30° overlayer is a mixed OH + H_2O rather than a pure Pt(111)−($\sqrt{3} \times \sqrt{3}$)R30°−2OH phase. On the other hand, HREELS has proven to be rather sensitive to small amounts of H_2O on Pt(111) and Pt(111)−(2 × 2)−O.[8,24] Since HREELS did not provide any evidence for the presence of H_2O in the ($\sqrt{3} \times \sqrt{3}$)R30° overlayer, this issue will remain elusive.

The oxygen atoms are laterally displaced from the on-top position by 0.10 Å. The occupation of on-top sites by the hydroxyl species induces a buckling in the first Pt layer in which the oxygen-coordinated Pt atoms are shifted upward by 0.06 Å, resulting in an averaged expansion of 0.04 Å of the first metal−metal interlayer spacing. This expansion is significantly larger than that (0.01 Å) found in the Pt(111)−(2 × 2)−O phase.[22] There is no buckling in the second Pt layer, and only a small (not significant) contraction of 0.01 Å was found in the second metal−metal interlayer spacing compared with the bulk value.

The structural configuration is indicative of the formation of hydrogen bonds between adjacent OH groups. The presence of hydrogen bonds in the OH overlayer was already proposed on the basis of recent HREELS measurements.[8] The present DFT calculations support this interpretation since the ($\sqrt{3} \times \sqrt{3}$)R30°−2OH overlayer is by 0.3 eV per OH group more stable than in the ($\sqrt{3} \times \sqrt{3}$)R30°−1OH overlayer. The OH groups form on Pt(111) either zigzag OH chains with ($\sqrt{3} \times \sqrt{3}$)R30° symmetry or six-member rings of hydrogen-bonded OH with (3 × 3) symmetry. Both surface overlayers have been identified with STM[25] and simulated with DFT calculations in the form of pseudo-STM images (cf. Figure 3). According to the DFT calculations, the hydrogen atoms at the OH groups are invisible in STM since the corresponding orbitals involving the H-states are energetically far away from the Fermi level. The difference in the appearance in STM images of ($\sqrt{3} \times \sqrt{3}$)-R30° and (3 × 3) is mainly caused by the slight, characteristic lateral displacements of the O atoms.

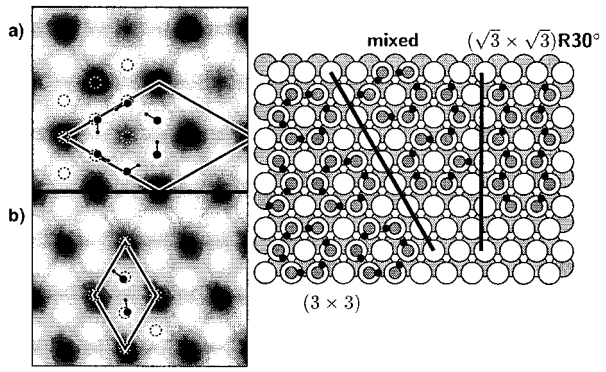

Figure 3. Simulated STM images of Pt(111)−($\sqrt{3} \times \sqrt{3}$)R30°−2OH and Pt(111)−(3 × 3)−6OH using the Tersoff−Hamann model. The honeycomb structure is apparent as in the experimental STM image. Hydrogen atoms are invisible in the pseudo-STM images. For comparison, the models used in the STM simulations are displayed. The ($\sqrt{3} \times \sqrt{3}$)R30°−2OH surface consists of zigzag OH chains, while the (3 × 3)-6OH phase reveals six-member rings of OH.

Chemisorbed OH acts electronically as an electron acceptor, i.e., the electron density is flowing from the Pt atoms toward the hydroxyl groups. This has been confirmed by our DFT calculations as the calculated work function of the hydroxyl covered Pt(111) surface increases indeed by 1 eV in comparison with the clean Pt(111) surface. The same conclusion was drawn from the calculations of OH on a Pt_6 cluster.[26] The experimental work function increase of OH on Pd(100) corroborates also the electron-accepting character of the adsorbed OH species.[27]

The DFT calculated Pt−O−H bond angle of 104.24° is almost identical to that in the H_2O molecule. In comparison with H_2O molecules, which are sp^3 hybridized, it is therefore plausible to assume that the oxygen atom of adsorbed OH on Pt(111) adopts also the sp^3 hybridization. The Pt−OH bond may therefore be regarded as replacing one of the O−H bonds in H_2O by an O−Pt bond. The unpaired electron of OH is then involved in the O−Pt bond formation, while one of the lone electron pairs of OH participates in the hydrogen bond with neighboring OH groups. As a consequence, the on-top adsorption is preferred for OH on Pt(111). The sp^3 hybridization of the oxygen atom also explains the bending of the O−H bond away from the surface normal, which intensifies the OH bending mode in HREELS.[1,8]

In the following, we examine the hydrogen bond of neighboring OH (OH_a and OH_b) on Pt(111) with DFT calculations by comparing the interaction density of Pt(111)−OH with that of H−OH (cf. Figure 4). The separation between the H−OH entities, the orientation of the OH, and the bond angle within each H−OH complex were chosen to be identical to those of the configuration of Pt(111)−OH. The interaction densities $\Delta\rho^i$

(22) Materer, N.; Starke, U.; Barbieri, A.; Doll, R.; Heinz, K.; Van Hove, M. A.; Somorjai, G. A. *Surf. Sci.* **1995**, *325*, 207.
(23) Michaelides A.; Hu, P. *J. Chem. Phys.* **2001**, *114*, 513−519.
(24) Bedürftig, K. Ph.D. dissertation, FU Berlin, Berlin, Germany, 1999.
(25) Völkening, S.; Bedürftig, K.; Jacobi, K.; Wintterlin, J.; Ertl, G. *Phys. Rev. Lett.* **1999**, *83*, 2672−2675.
(26) Fahmi, A.; van Santen, R. A. *Z. Phys. Chem.* **1996**, *197*, 203.
(27) Nyberg, C.; Tengstal, C. G. *J. Chem. Phys.* **1984**, *80*, 3463.

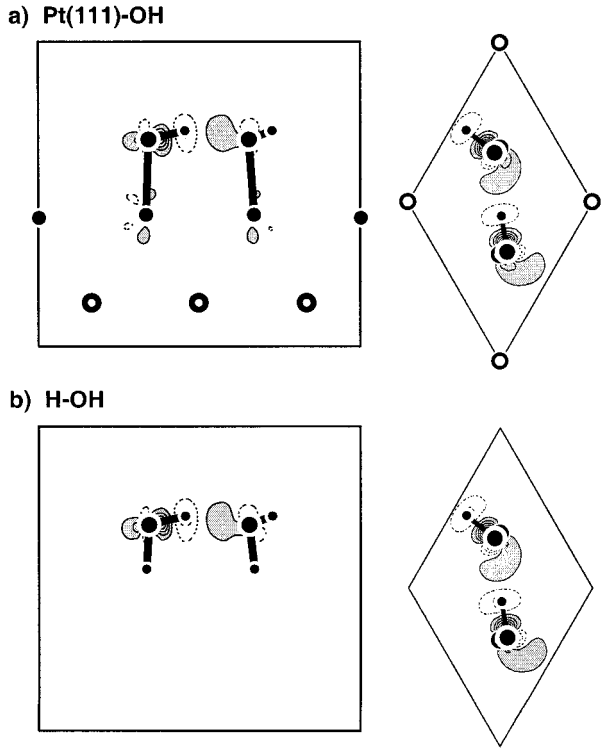

Figure 4. The interaction density of 2OH on Pt(111) in comparison with two H_2O in a corresponding geometry (left: side view, right: top view). For the definition of the interaction density the reader is referred to the text. In both cases the interaction between the OH groups is driven by hydrogen bonds, and according to the interaction density plots these are identical for both cases. The OH−OH interaction causes the lone-pair orbital to accumulate even more electron density, while the H end becomes electron depleted.

are given by differences of electron densities ρ of the corresponding systems as

$$\Delta\rho^{i}[\mathrm{H{-}OH}] = \rho[(\mathrm{H{-}OH})_a{+}(\mathrm{H{-}OH})_b] - \rho[(\mathrm{H{-}OH})_a] - \rho[(\mathrm{H{-}OH})_b]$$

and

$$\Delta\rho^{i}[\mathrm{Pt{-}OH}] = \rho[\mathrm{Pt(111){-}2OH}] - \rho[\mathrm{Pt(111){-}OH_a}] - \rho[\mathrm{Pt(111){-}OH_b}] + \rho[\mathrm{Pt(111)}]$$

The interaction density vanishes per definition if there is no interaction between the OH groups bonded either to H or to Pt(111). However, the interaction density is nonzero for interacting OH groups, indicating a mutual polarization. It is somewhat surprising that the interaction densities of H−OH and Pt(111)−OH in Figure 4 are identical, implying that also the hydrogen bonding between OH groups on Pt(111) and that between water molecules is identical. The interaction-induced polarization within the OH group is described by a gain of electron density in one of the lone-pair orbitals and depletion in the electron density at the H end. This polarization pattern promotes the electrostatic attraction between the hydrogen atom and the lone-pair orbital of the adjacent OH group. We estimated the electrostatic dipole−dipole interaction to be attractive by 0.34 eV per molecule, very close to the total interaction energy of the two hydroxyls (0.30 eV). Thus, the main contribution to the interaction is concluded to be electrostatic, and the remaining difference might be due to Pauli repulsion between the orbitals of the hydroxyl groups.

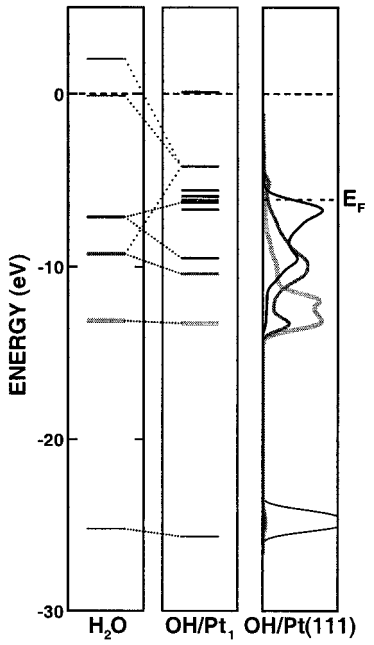

Figure 5. The level diagram of H_2O (left), OH interacting with a single Pt atom (middle), and the overlap of the molecular orbitals of water with those of OH/Pt(111) (right) broadened with a Gaussian of width 0.35 eV. The dashed lines show the corresponding hybrids in the finite systems, and the Fermi level of Pt(111) is indicated at the right-most panel. The zero of the energy is set to the vacuum level.

The discussion about the interaction density suggests that the bonding of OH on Pt(111) is essentially identical to that of OH to a single H atom in H_2O. To further support this view, the hybridization of the orbitals of the hydroxyl with the states of a single Pt atom and the Pt(111) are compared to those of water (cf. Figure 5). First, the hydroxyl levels in Pt_1OH closely resemble the water levels when the bonding and antibonding hybrids of the OH-p_x with the Pt-d_{xz} are taken into account. Second, the levels of the OH/Pt(111) match well those of the hybrid orbitals of Pt_1OH. Thus, the bonding of OH to the Pt(111) surface is indeed similar to the bonding to the hydrogen in a water molecule and the difference is well understood.

Experimentally we prepared also a $(\sqrt{3} \times \sqrt{3})$R30° overlayer on Pt(111) by exposing 0.5 L of H_2O at 100 K. From TDS the H_2O desorption peak is significantly lower (about 30 K) than that of the $(\sqrt{3} \times \sqrt{3})$R30°−2OH, indicating different overlayer phases. The HREELS data of these two $(\sqrt{3} \times \sqrt{3})$R30° phases are also substantially different and were interpreted in terms of pure OH and H_2O overlayers, respectively.[24] However, the LEED I−V data of the $(\sqrt{3} \times \sqrt{3})$R30°−$H_2O$ are identical to those of the Pt(111)−$(\sqrt{3} \times \sqrt{3})$R30°−OH surface. Using LEED as the fingerprinting technique,[28] this finding tells us that also the O skeleton and the adsorption site in both phases must be identical.

Conclusions

The coadsorption of water on a (2×2)−O precovered Pt(111) surface at 100 K and subsequent annealing to 155 K led to a well-ordered overlayer with $(\sqrt{3} \times \sqrt{3})$R30° periodicity. The atomic structure of the O skeleton was determined by full

(28) Over, H.; Gierer, M.; Bludau, H.; Ertl, G.; Tong, S. Y. *Surf. Sci.* **1994**, *314*, 243.

dynamical LEED calculations; recall that LEED is insensitive to hydrogen. There are two O-containing groups per ($\sqrt{3} \times \sqrt{3}$)R30° unit cell and both are sitting in near on-top positions. The Pt−O bond length is (2.11 ± 0.04) Å. The LEED results are substantiated by the density functional theory (DFT) calculations. Assuming that the O-containing species is OH, the positions of oxygen and hydrogen clearly indicate hydrogen bonds between the adjacent OH groups. The bonding of OH to Pt(111) is shown to be similar to that of OH in H_2O, i.e., the O atoms constitute an sp^3 hybridized center.

Acknowledgment. Y. J. Zhu appreciated the financial support by the Alexander von Humboldt Foundation as a research fellow. The ZIB is acknowledged for providing Cray-T3E computing time.

JA015525L